

Mapping Polymeric Properties using Combinatorial and High-Throughput Methods: Adhesion and Mechanical Properties*

Aaron M. Forster, Arnaud Chiche, Martin Y. M. Chiang, Christopher M. Stafford, Alamgir Karim
Polymers Division
National Institute of Standards and Technology, Gaithersburg, MD, USA

Introduction

The NIST Combinatorial Methods Center (NCCM) develops Combinatorial and High-Throughput (C&HT) methods for material properties measurements. C&HT methods combine experiment design, instrument automation, and computing tools to form a new paradigm for scientific research. Through this combination of disciplines, combinatorial methods provide a faster and more comprehensive exploration of complex parameter spaces. Given this premise, the C&HT concept is being adapted by the NCCM to achieve similar benefits in materials science.

The pharmaceutical and genomics industries have benefited from utilizing combinatorial techniques for the discovery of new products. However, the C&HT methods developed for the pharmaceutical industry often cannot be applied directly to materials research since methods for generating materials libraries and for rapidly measuring properties, especially adhesive or mechanical properties, are often lacking.

A current focus of the NCCM is the development of novel high-throughput platforms for both adhesion and mechanical property testing. This presentation will describe four different C&HT methods that have been developed at NIST specifically to fill the need for adhesive and mechanical properties testing platforms.

Multi-lens Adhesion Measurements

Adhesive contact tests provide a method to probe the effect of interfacial characteristics important to adhesion such as chemical bonding, roughness, or mechanical interlocking. The Johnson, Kendall, and Roberts (JKR) test utilizes a single hemispherical lens compressed against (loading) and removed from (unloading) a substrate. The JKR theory models the contact behavior between two elastic solids to account for adhesive forces as a function of contact area, contact geometry, and load or displacement. The NCCM has adapted the JKR test to develop a high-throughput adhesion measurement platform.^[1] This test utilizes an array of hemispherical lenses, rather than a single lens, to conduct multiple adhesion tests during one loading/unloading cycle. A schematic of the lens array along with the multi-lens JKR test apparatus is given in Figure 1a.

Essential to the quantification of adhesion energies with the JKR equation is the measurement of two of three variables: load, contact area, and displacement. Typically, the contact area and load are measured during the test and

this data is fit to the JKR equation to determine E and G , the system modulus and energy release rate, respectively.^[2] Experimentally, displacement is not used due to difficulties in determining the initial contact point. In the case of linear elastic deformation and contact equilibrium, G is equal to the thermodynamic work of adhesion. For the multi-lens adhesion test, where the load on each lens is not available, calculations can be performed with respect to the strain energy release rate.^[2]

$$G = \frac{2E(\delta' - \delta)^2}{3\pi a} \quad (1)$$

where E is the lens modulus, δ is the lens displacement, a is the contact area, and $\delta' = a^2/R$ is the displacement required to establish a contact radius of a without the presence of surface or adhesion forces.^[2] This value represents the energy required to change the contact area by a unit amount. The strain energy release rate is not constant, but depends on the rate at which the contact area changes during unloading.

Results and Discussion

Figure 1b shows the strain energy release rate as a function of contact radius measured for a single glass lens against a polydimethylsiloxane (PDMS) film. The solid lines are the strain energy release rate calculated from two potential displacement points of initial contact for the lens against the PDMS film. As seen from Figure 1, the uncertainty in the initial contact point may create a large difference between the load and displacement determined strain energy release rate. The question we attempt to answer is whether a multi-lens test, with displacement rather than load measurements, will better match the strain energy release rate calculated from a single lens measurement using displacement values. This process will determine the validity of the multi-lens test as a high-throughput adhesion measurement technique. In this presentation, multi-lens adhesion tests will be compared to single lens tests to determine the potential for utilizing displacement of the multi-lens array as an experimental variable to quantify strain energy.

Combinatorial Peel Tests

The peel test is one of the most common techniques to investigate the properties of pressure sensitive adhesives

(PSA).^[3] We investigate the potential and limitations of a high throughput peel test by probing different parameters, for example adherent roughness and surface energy, peel rate, adhesive and backing thickness. The primary focus is on the mechanisms which control adhesive debonding, in particular relating to the effects of the adherent surface energy on the peel force and mechanism.

Results and Discussion

We perform 90° peel experiments with a custom designed apparatus. A commercial transparent adhesive tape (Scotch 600 from 3M. Tape width b is 1.9 mm),^[4] is applied on the adherent surface at room temperature with a commercial 2 kg (4.5 lb) roller (diameter 9.5 cm and width 4.5 cm, from ChemInstruments^[4]). The peel test was performed within a few minutes after application to the adherent. We have investigated two model adherent surfaces. The first, which functions as a reference, consists of a regular glass slide (75 mm length), initially covered with a grafted monolayer of a short alkyl silane chain of *n*-octadecyldimethylchlorosilane (ODS). It exhibits a homogeneous low surface energy of 26 mJ/m². A second surface was prepared by symmetric UVO gradient exposure of the reference surface and washed with toluene, as described elsewhere.^[5]

The evolution of the force F (divided by the tape width b) is shown in Figure 2 for both of the prepared samples. In the case of a homogeneous ODS surface (gray curve), the force is constant at a value of 26 N/m \pm 1 N/m (error bar represents one standard deviation of the data, and is taken as the uncertainty of the measurement). In the case of the gradient surface (black curve), large variations are observed, from almost 30 N/m where the ODS layer is nearly unmodified (zero exposure time) to 190 N/m where the exposure time is the highest (40 s) and so the surface energy of the adherent is also highest (Figure 2, top). The relation between peel force and exposure time (therefore surface energy) emerges clearly: increasing the UVO exposure time linearly increases the peel force.

The symmetry of the load variation along the sample (Figure 2, black curve) also suggests that the result of the test is not sensitive to the peel direction relative to the energy gradient. This is not necessarily true in other systems or gradients including, for example, the case of a thick (or stiff) adhesive layer, due to the potential variation of substrate properties within the contact edge width.

Edge-Delamination Test

In the proposed combinatorial edge delamination test, a film is flow-coated onto a relatively rigid substrate such that the film has a thickness gradient in one direction (Figure 3a). The film and substrate are diced into a square grid pattern to form an array of individual edge delamination samples on the substrate (Figure 3b). The edges are at 90° to the interface of the film/substrate. The depth (d) and width (w) of the cut (Figure 3c) are the design parameters that need to be optimized and have been discussed in a

previous publication.^[6] Due to the existence of residual biaxial stresses during the solidification of the film and the stress-free edges after dicing in a bi-material system, stress concentrations arise at the interface near the free edges. These stress concentrations are sufficient to create small initial interfacial flaws (cracks) at the film/substrate boundary and signifies the well-known free-edge effect that is unique to bi-material systems.^[7] To introduce loading of these interfacial flaws, the specimen is cooled with a temperature gradient applied in the direction orthogonal to the thickness gradient (Figure 3a). During cooling, the coefficient of thermal expansion mismatch between the substrate and the polymer film increases stresses on these initial cracks. Interfacial debonding events will be observed for those samples having critical stresses that depend on the combination of local temperature and film thickness. Consequently, a failure map as a function of temperature and film thickness can be constructed with one step, as shown in Figure 3a. In principal, if the adhesion of a film to a substrate is independent of temperature, the adhesion can be deduced from this failure map as long as the thermo-mechanical property (the stress-temperature relation) of the test film is well characterized.^[8]

Results and Discussion

In order to demonstrate the variability of the proposed combinatorial methodology, a single specimen of a thin PMMA film bonded to a substrate with orthogonal film thickness and contact angle gradients was subdivided into separate samples. The contact angle (θ_c) gradient on the substrate was introduced by modifying the contact angle of a self-assembled monolayer (SAM) generated on the substrate. The film thickness ranges from 3.66 μ m to 9.11 μ m over a 30 mm distance. Contact angle ranges from 23.1° and 68.3° over a 50 mm distance. Within experimental uncertainties, separate measurements of thickness and contact angle show that both have a linear variation within the specimen. After cooling the specimen, having 104 individual edge delamination samples, debonding events were observed for those samples having the critical relationship of the stress and adhesion as shown in Figure 4a. By tracing the locus of far-field debonding, a failure map as a function of film thickness and contact angle was constructed. Figure 4b gives the quantitative information of the critical relationship between the h_f and θ_c .

SIEBIMM Method

We have developed a HT method for measuring the mechanical properties of polymer thin films based on a wrinkling instability in bilayers and laminates.^[9] Indeed, this technique is very simple and practically any laboratory, academic or industrial, can perform such measurements with only modest investment in equipment.

This measurement platform exploits a classic mechanical instability that occurs in laminates and sandwich structures under compression. In the geometry described here, a periodic buckling instability arises from a

mismatch of the elastic moduli of a relatively stiff polymer coating that has been applied to a soft silicone substrate (i.e. PDMS). Either conventional light scattering or optical microscopy is used to rapidly measure the wavelength of the wrinkles. In addition, the sample can be rastered across the beam to map out the properties of the entire film if the sample is comprised of a gradient library, or if the sample is uniform, a multitude of images can be acquired to generate sufficient statistics. We have denoted this technique as Stain Induced Elastic Buckling Instability for Mechanical Measurements (SIEBIMM). Since this is an intrinsically local measurement, this technique is well suited for measurements of combinatorial libraries with spatially varying properties that can be prepared by existing methodologies developed at NIST.

Results and Discussion

The dependence of the buckling wavelength on the material properties of both the stiff upper film and the soft substrate has been established.^[10] Upon compression, the energy required to bend the stiff upper film is balanced against the energy needed to deform the substrate. This derivation assumes that there is sufficient adhesion between the two materials to transfer stress across the interface as well as suppress delamination. The relationship between the buckling wavelength and the system properties can be written as follows:

$$E_f = 12E_c \left[(3 - \nu_c)(1 + \nu_c) \right]^{-1} [d / 2\pi h]^3 \quad (2)$$

where E_f and h are the modulus and thickness of the stiff upper film, E_c and ν_c are the modulus and Poisson's ratio of the soft substrate, and d is the wavelength of the sinusoidal buckles.

As a demonstration of the quantitative nature of SIEBIMM, two polystyrene films were prepared by spin coating from dilute solution. The thickness of each film was determined by x-ray reflectivity (XR) to be $59.7 \text{ nm} \pm 0.5 \text{ nm}$ and $30.7 \text{ nm} \pm 0.5 \text{ nm}$, respectively. The films were transferred to PDMS and subjected to a compressional strain of 4 %. For the thinner film, the wavelength was too small to measure by light scattering. Therefore, atomic force microscopy (AFM) images were obtained in order to accurately measure the buckling wavelength. The AFM images ($25 \mu\text{m} \times 25 \mu\text{m}$ scans) of the buckled 59.7 nm film and 30.7 nm film are shown in Figures 5a and 5b, respectively. Image analysis of these AFM micrographs yields quantitative results for this simple demonstration. The wavelength of the image in Figure 5a was found to be $3.38 \mu\text{m}$, while the wavelength in Figure 5b was found to be $1.74 \mu\text{m}$. Using Equation 2, the modulus of the 59.7 nm film is calculated to be $3.1 \text{ GPa} \pm 0.3 \text{ GPa}$, while the modulus of the 30.7 nm film is found to be $3.1 \text{ GPa} \pm 0.2 \text{ GPa}$. These results are in excellent agreement with previous results for thicker films ($300 \text{ nm} > h > 100 \text{ nm}$) that displayed a modulus of $3.2 \text{ GPa} \pm 0.1 \text{ GPa}$.

Conclusions

Several C&HT techniques have been presented for the measurement of adhesive and mechanical properties. Each test is designed to probe a specific material property, but all are scalable to the investigation of combinatorial libraries. In this presentation, we discuss the latest developments within C&HT adhesion and mechanical property measurements.

Acknowledgements

CMS and AMF acknowledge support from the NIST National Research Council Postdoctoral Fellowship Program. CMS also acknowledges Bryan Vogt for XR measurements. AC would like to thank Patricia McGuiggan for helpful advice.

* Contribution of the National Institute of Standards and Technology, not subject to copyright in the United States.

References

1. Crosby, A. J.; Karim, A.; Amis, E. J., *J. Polym. Sci. Pol. Phys.*, **41**, 883-891 (2003).
2. Shull, K. R., *Mat. Sci. Eng. R*, **36**, 1-45, (2002).
3. D. Satas, *Handbook of pressure-sensitive adhesive technology*, Van Nostrand Reinhold, New York, (1982).
4. Equipment and instruments or materials are identified in the paper in order to adequately specify the experimental details. Such identification does not imply recommendation by NIST, nor does it imply the materials are necessarily the best available for the purpose.
5. S. V. Roberson, A. J. Fahey, A. Sehgal, A. Karim, *Appl. Surf. Sci.*, **200**, 150-164, (2002).
6. M. Y.M. Chiang, W. L. Wu, J. He, E. J. Amis, *Thin Solid Films*, **437**, 197-203, (2003).
7. D. B. Bogy, *J. of Applied Mechanics*, **35**, 460-466, (1968).
8. E. O. Shaffer, F. J. McGarry, L. Hoang, *Poly. Eng. and Sci.*, **36**, 2375, (1996).
9. C.M. Stafford, C. Harrison, A. Karim, E.J. Amis, *Polymer Preprints*, **43**, 1335, (2002).
10. H.G. Allen, *Analysis and Design of Structural Sandwich Panels*, Pergamon Press, New York, (1996).

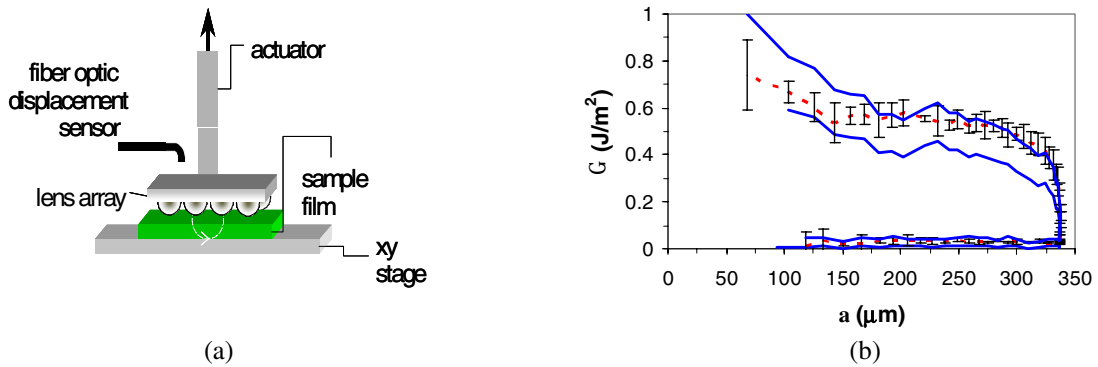


Figure 1. a) Schematic of the multi-lens array apparatus. The lens contact area is imaged from below through an inverted microscope. b) The solid lines represent the strain energy release rate calculated from equation 1 at the upper and lower displacement uncertainty bounds. The dotted line is the strain energy release rate calculated from the load values.

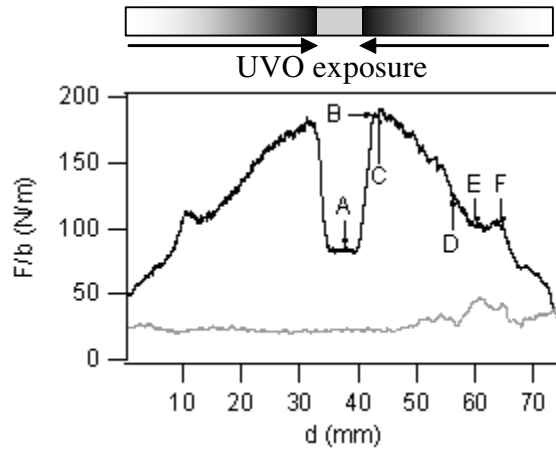


Figure 2. Evolution of the peel force F/b with the edge displacement d during the peeling of the adhesive tape from a glass slide grafted with ODS. The gray curve corresponds to a homogeneous surface, the black one to the surface with energy gradients. Top: schematic of the UV exposure time associated with the black curve.

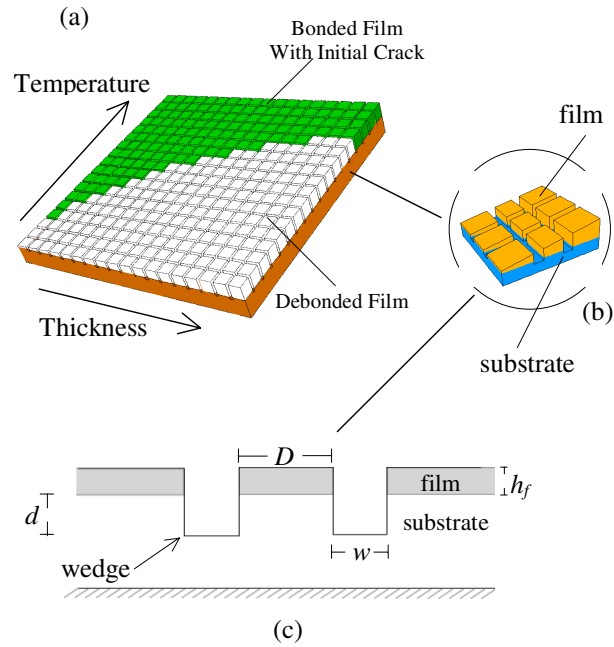


Figure 3. A schematic of the combinatorial approach to the edge lift-off test: (a) the multivariate specimen with film thickness and temperature gradients, and final failure map; (b) a square pattern array of individual edge delamination samples on the substrate; (c) the cutting depth, d , and width, w .

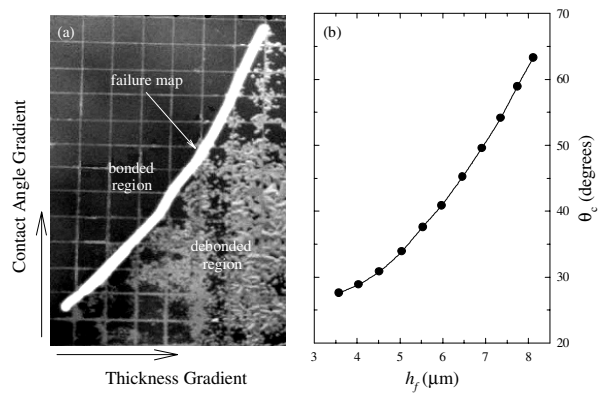
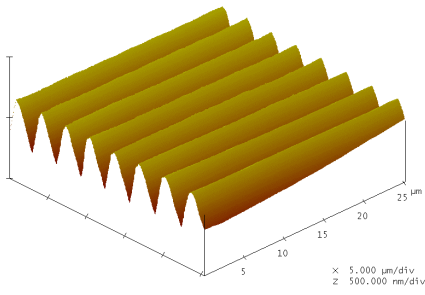
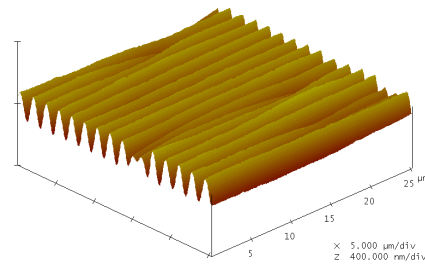


Figure 4. (a) Debonding events in a typical combinatorial edge delamination specimen having PMMA film bonded to the silicon substrate. (b) the variation of contact angle with the film thickness along the failure map.



(a)



(b)

Figure 5. a) AFM micrograph of a buckled film of polystyrene, having a thickness, h , of $59.7 \text{ nm} \pm 0.5 \text{ nm}$, supported by and adhered to PDMS. b) AFM micrograph of a buckled film of polystyrene, having a thickness, h , of $30.7 \text{ nm} \pm 0.5 \text{ nm}$, supported by and adhered to PDMS.